

1 **Supplementary Material for “Direct ecosystem fluxes of**  
2 **volatile organic compounds from oil palms in South-East**  
3 **Asia”**  
4

5 **P. K. Misztal<sup>1,2\*</sup>, E. Nemitz<sup>1</sup>, B. Langford<sup>1</sup>, C. Di Marco<sup>1</sup>, G. J. Phillips<sup>1#</sup>, C. N.**  
6 **Hewitt<sup>3</sup>, R. MacKenzie<sup>3</sup>, S. M. Owen<sup>1</sup>, D. Fowler<sup>1</sup>, M. R. Heal<sup>2</sup> and J. N. Cape<sup>1</sup>**

7 [1]{Centre for Ecology & Hydrology, Penicuik, EH26 0QB, UK}

8 [2]{School of Chemistry, University of Edinburgh, EH9 3JJ, UK}

9 [3]{Lancaster Environment Centre, Lancaster University, LA1 4YQ, UK}

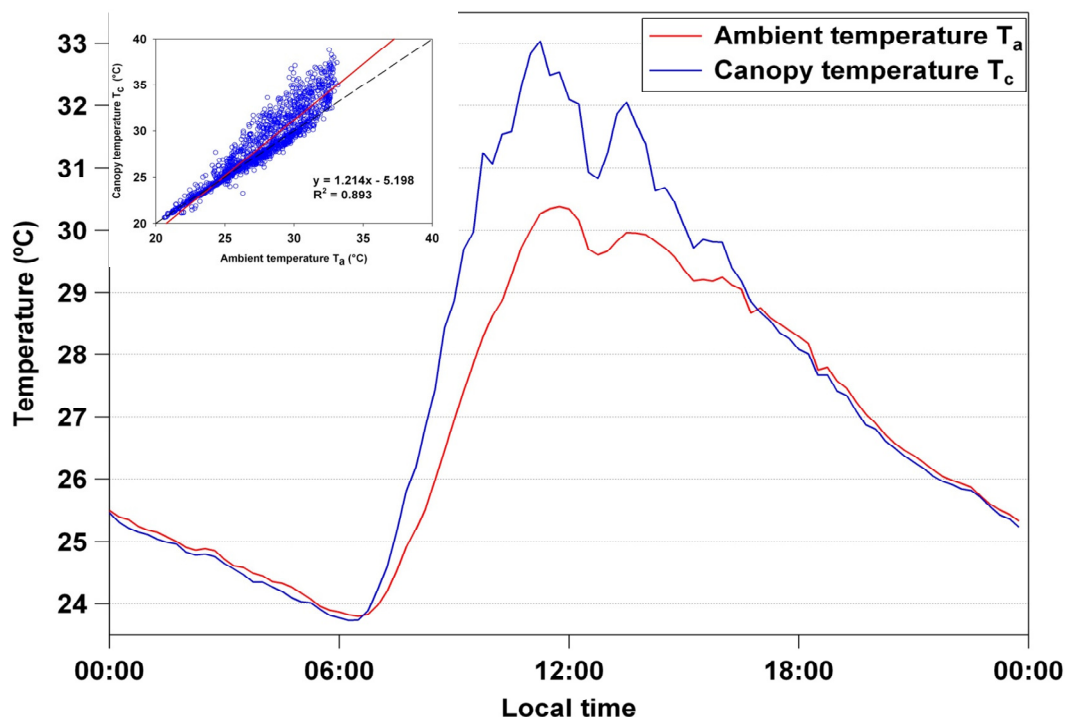
10 \* Currently at Department of Environmental Science, Policy, and Management, University of  
11 California, Berkeley, CA, US

12 # Now at NCAS, School of Earth and Environment, University of Leeds, UK.

13 Correspondence to: P.K. Misztal (pkm@berkeley.edu)

14  
15 **SI-1 Ambient and canopy temperature**

16 Figure S1 shows diurnal patterns of measured ambient temperature and the average canopy  
17 temperature estimated from extrapolation of the ambient temperature to the surface, using the  
18 sensible heat flux and the resistance approach (Nemitz et al., 2009).



1

2 Figure S1. Comparison between the ambient ( $T_a(15\text{ m})$ ) and canopy ( $T_c$ ) temperature estimated from  
 3 resistance approach showing  $T_c$  higher by approximately  $2\text{ }^\circ\text{C}$  during the midday and lower by  $0.2\text{ }^\circ\text{C}$   
 4 at night. Inset shows regression and higher variability of  $T_c$  in the upper temperature range.

5

## 6 SI-2 Proton Transfer Reaction Mass Spectrometry (PTR-MS)

7 The concentrations and eddy fluxes of biogenic volatile organic compounds (BVOCs) were  
 8 measured by a Proton-Transfer-Reaction Mass Spectrometer (PTR-MS) operated in  
 9 continuous flow disjunct eddy covariance (cfDEC) mode, also referred to as the virtual  
 10 disjunct eddy covariance (vDEC) mode, described in the next section. The instrument was the  
 11 high-sensitivity model (Ionicon, Austria, s/n 04-03) which was equipped with an additional  
 12 turbomolecular pump for the detection chamber and incorporated Teflon®, instead of Viton®,  
 13 gaskets in the drift tube. Since the characteristics of instrument design and operation have  
 14 been thoroughly described in the literature (Blake et al., 2009; de Gouw, 2007; Hansel et al.,  
 15 1995; Lindinger et al., 1998; Warneke et al., 2001), only a general overview specific to  
 16 running at high humidity will be given here.

17 The principle of PTR-MS is the soft ionisation of VOCs by hydronium ions formed in a  
 18 hollow cathode ion-source from pure water vapour; these effectively transfer protons to all

1 molecules with proton affinities (PA) greater than that of water. Most VOCs have sufficiently  
2 large PA for effective ion transfer, but a few low-weight molecular compounds, with PA only  
3 slightly higher than water (e.g. formaldehyde), may require specific optimisation to minimise  
4 the impact on sensitivity of humidity dependent back-reactions. The conditions inside the  
5 reaction chamber are dependent on both electric field ( $E$ ) and the number density of the buffer  
6 gas ( $N$ ) and the ratio of these ( $E/N$ ) determines the degree of fragmentation and clustering. At  
7 typical ambient conditions this ratio is kept in the range 120 – 140 Td ( $1 \text{ Td} = 10^{-17} \text{ V cm}^2$ ).  
8 However, for a constant  $E/N$  ratio the sensitivity is proportional to  $N$  and thus operation at 2  
9 mbar or larger is recommended (Warneke et al., 2001). The protonated ions are filtered  
10 through a quadrupole mass filter (QMA 400) and counted with a Secondary Electron  
11 Multiplier (Pfeiffer SEM-217) coupled to an ion-count preamplifier (Pfeiffer CP-400). The  
12 radio frequency and direct current are generated by an RF box (Pfeiffer QMH 400). Since the  
13 sampled VOCs undergo protonation, they are detected at a mass to charge ( $m/z$ ) ratio equal to  
14 one unit greater than their molecular weight. The soft ionisation method means that most  
15 compounds can be detected as their parent ion. For heavier compounds ( $m/z >100$ ) the  
16 protonated masses reflecting two or more fragments may need to be taken into account. This  
17 is the case, for example, for monoterpenes ( $m/z$  137, 81) (e.g. Tani et al., 2003) and  
18 sesquiterpenes ( $m/z$  205, 149) (Kim et al., 2009). Because some compounds fragment more  
19 than others, appropriate calibration and calculation approaches have to be applied (sections  
20 SI-3 and SI-5).

21 The optimisation of the PTR-MS and the sampling system sought a compromise between  
22 reliable measurements at very high humidity and sensitivity for VOCs. Tani et al. (2004)  
23 showed that sample humidity has a significant impact on fragmentation patterns at normal  
24  $E/N$  ratios, but has no influence if  $E/N$  is kept around 140 Td. The water vapour pressures  
25 tested by these authors ranged from 0.59 to 2.4 kPa. However, the vapour pressures  
26 encountered at the oil palm site were much higher, ranging from 2.5 to 3.2 kPa (2.75 kPa on  
27 average) due to high relative humidity (88% on average) accompanied by high temperatures  
28 (22 – 31 °C). Humidity effects on PTR-MS measurements were also studied by Warneke et  
29 al. (2001), who noted decreasing sensitivities at higher humidities, although again the levels  
30 of specific humidity encountered in Borneo were not tested by these authors. Although the  
31 sensitivity could be enhanced by increasing the drift tube pressure to 2 - 3 mbar this approach  
32 was not possible for the conditions here, because the high flow in the sampling line and the  
33 high specific humidity would have required operation at a detection pressure close to or above

1 the set points of the instrument. In addition, higher drift tube pressure would have increased  
2 the likelihood of internal condensation.

3 Therefore, the optimal operating conditions were determined experimentally to be a drift tube  
4 pressure of 1.6 mbar, inlet and drift-tube temperatures of 45 °C and drift voltage of 485 V,  
5 giving an  $E/N$  value of 140 Td. This was maintained constant throughout the experiment. Our  
6 subsequent measurements in the laboratory revealed less than 5% reduction in sensitivity  
7 when operating at 1.6 mbar drift tube pressure, compared to 2.2 mbar at the same  $E/N$  ratio.  
8 However, high ambient water vapour pressure had an additional impact on the sensitivities,  
9 and normalisation for the presence of water clusters was required (Davison et al., 2009; Tani  
10 et al., 2004). The overall reduction in sensitivity was estimated at 20% with respect to  
11 operation at temperate humidities.

12 The system was automated to run continuously in 3 modes: (1)  $m/z$  21-206 scan of ambient  
13 air; (2) multiple ion detection (MID) of 11 pre-selected VOCs at 0.5 s dwell time each (0.2 s  
14 for additional  $m/z$  21 and 37 corresponding to  $\text{H}_3^{18}\text{O}^+$  and  $\text{H}_3^{16}\text{O}(\text{H}_2^{16}\text{O})^+$ , respectively; and  
15 (3)  $m/z$  21-206 background measurement of humid VOC-free air. Mode 1 was set to run for  
16 the first 5 minutes of each hour, then 25 min was devoted to mode 2, then mode 3 for 5 min  
17 and again mode 2 for the remaining 25 min. The switching between modes was automated  
18 through a solenoid valve system operated from the 12 V DC power port of the PTR-MS  
19 power supply unit and managed through a QS422 sequence. The online preview and logging  
20 of volume mixing ratios and fluxes was done using the DDE feature of the Balzer sequencer  
21 communicating with a LabVIEW program which logged the sonic anemometer data together  
22 with the PTR-MS data to one file, so that each 25-min file contained 30000 rows of wind  
23 data, 210 of which also contained PTR-MS data which were synchronised in time, but not yet  
24 corrected for the lag-time associated with the residence time in the tubing (see Sect. SI-5).

25 Direct calibration used a VOC gas mixture supplied by Apel-Riemer Environmental Inc.,  
26 USA, which contained methanol, acetaldehyde, acetone, isoprene, acetonitrile and  
27 formaldehyde, each at 1 ppmv, and d-limonene at 0.18 ppmv. The standard was diluted on  
28 site with the same zero air from a custom-built generator containing Pt/Al<sub>2</sub>O<sub>3</sub> catalyst heated  
29 to 250 C (Misztal et al., 2010), as the zero air used for mode 3. The catalyst worked  
30 efficiently for all VOCs including methanol and provided humidity similar to the ambient. It  
31 was used at the site to dilute high concentration standard into clean Tedlar® bags using new  
32 high quality gas-tight syringes; the bags were prepared freshly just before the calibration. The

1 calibration range was broad from 20 pptv to 500 ppbv ensuring high precision and minimizing  
 2 any potential artefacts from using the Tedlar ® bags. The subsequent calibration in the lab at  
 3 the same drift conditions but with much less humid air revealed that the high humidity  
 4 contributed to approximately 20% lower sensitivities in the field. The standard was checked  
 5 after the campaign by reference to a GC-MS calibrated with a different isoprene standard  
 6 (BOC gases, UK) and a d-limonene standard prepared from a diluted (with methanol) liquid  
 7 standard (Sigma Aldrich, UK) injected directly onto the column. Agreement for isoprene and  
 8 monoterpenes was within 4% and 10%, respectively. The other VOCs were compared with  
 9 another gas standard delivered by Apel-Riemer (at 0.5 ppm concentration per VOC) which  
 10 was 2 years older and contained the same VOCs plus MVK, and other organics. The  
 11 agreement was within 18%; the older standard showed 8-18% smaller concentrations for all  
 12 VOCs except for acetaldehyde, which was 8% higher possibly through contributions of  
 13 fragments from other organic species (e.g. MVK) that were not present in the other mixture. It  
 14 has been assumed that the calibration standard was within the certified 5% standard precision  
 15 for isoprene and other VOCs at the time of calibration. A larger uncertainty of 20% has been  
 16 attributed to MVK sensitivity, which was not present in the calibration standard in the field,  
 17 but which was inferred from the comparison of the sensitivity curves in the laboratory derived  
 18 from the MVK containing standard. It was also assumed that the sensitivity for the sum of  
 19 MVK+MACR is the same as for MVK only.

20

### 21 **SI-3 Derivation of volume mixing ratios (VMRs)**

22 The signal intensities measured as counts per second  $I_{m/z}$  (cps) for each of the monitored  $m/z$   
 23 channels were first converted to normalised counts per second  $I_{m/z}$  (ncps) (Davison et al.,  
 24 2009) in order to compensate for fluctuations in the primary ion, water vapour and drift-tube  
 25 pressure.

$$26 \quad I_{m/z} (ncps) = \frac{I_{m/z} (cps) \times 10^6}{I_{21} (cps) \times 500 + I_{37} (cps) + I_{55} (cps)} \times \frac{P_{dnorm}}{P_d},$$

27 (S1)

28 where  $I_{21}$ ,  $I_{37}$  and  $I_{55}$  are the instantaneous counts (cps) of  $H_3^{18}O^+$  (approximately a factor of  
 29 500 lower than  $H_3^{16}O^+$ ),  $H_3^{16}O(H_2^{16}O)^+$ , and  $H_3^{16}O(H_2^{16}O)_2^+$ , respectively. The  $m/z$  21  
 30 channel instead of  $m/z$  19 was selected for monitoring the primary ions in order to prevent

1 detector saturation. Generally a natural  $^{16}\text{O}/^{18}\text{O}$  isotope ratio of 500 is used in the calculation  
2 (Kuhn et al., 2007; Langford et al., 2009a) although the use of a slightly lower precise ratio of  
3 487 was proposed (Taipale et al., 2008). In fact, the true ratio might differ slightly depending  
4 on the location (e.g. close to oceanic waters) and one of the purposes of normalisation is to  
5 make the results uniform for comparisons with other results, where the level of primary ions  
6 used was different. In our case the level of primary ion counts was  $6.5\text{-}7.5 \times 10^6$  cps. The  
7 volume mixing ratios ( $\chi$ ) were obtained for each VOC as:

$$\chi_{\text{VOC}} = \frac{I_{m/z}(\text{ncps}) - I_{m/z(\text{zero})}(\text{ncps})}{S_{m/z}(\text{ncps/ppbv})} \quad .$$

8  
9 (S2)

10 Here,  $I_{m/z(\text{zero})}(\text{ncps})$  is the background normalised count rate for the given  $m/z$  channel, and the  
11  $S_{m/z}(\text{ncps/ppbv})$  is the normalised sensitivity for a given compound. The  $S_{m/z}$  for compounds  
12 present in the gas standard was obtained from the slope of a 6-point calibration line in the  
13 range 0 to 500 ppbv (0 to 90 ppbv for monoterpenes) corrected for background  $I_{m/z}(\text{ncps})$ .

14 The standard was appropriately diluted in clean Tedlar bags using VOC-free air, generated by  
15 purging ambient air through a Pt/ $\text{Al}_2\text{O}_3$  catalyst heated to 200 °C. This catalyst removed most  
16 VOCs effectively, but did not significantly affect water vapour concentrations, thereby  
17 avoiding problems arising from using dry calibration gas. However, normalisation for water  
18 clusters was always performed (Eq. S1). For compounds not present in the standard, the  
19 empirical sensitivity  $S'_{m/z}$  was approximated from the relative transmission curve (RTC)  
20 (Davison et al., 2009; Taipale et al., 2008). Only the sensitivities of non-fragmenting  
21 compounds which are known not to deviate significantly from the RTC (e.g. methanol,  
22 acetaldehyde, acetone, acetonitrile) were used to derive the relationship between the  
23 sensitivities and the transmission coefficients from using the reaction rate coefficients for the  
24 proton transfer reaction taken from Zhao and Zhang (2004). Since no large  $m/z$  compounds  
25 were used in calibration, the RTC approach was limited to the 21-71 range, and was extended  
26 later after comparison to the classical transmission coefficients using higher MW compounds  
27 such as xylene and camphor. The calibration error using the standard is assumed to be less  
28 than 5% while that from using reaction rate constants can be up to 100% (Steinbacher et al.,  
29 2004). However, the relative transmission approach used here can offer less than 30% relative  
30 error (Taipale et al., 2008). Table S1 summarises the actual sensitivities for compounds  
31 reported in the paper.

1 Table S1. Sensitivities for targeted compounds measured at oil palm. The values were derived  
 2 in calibration at the site, except for the values marked with an asterisk, which were obtained  
 3 using the relative transmission approach combined with calibration in the laboratory.

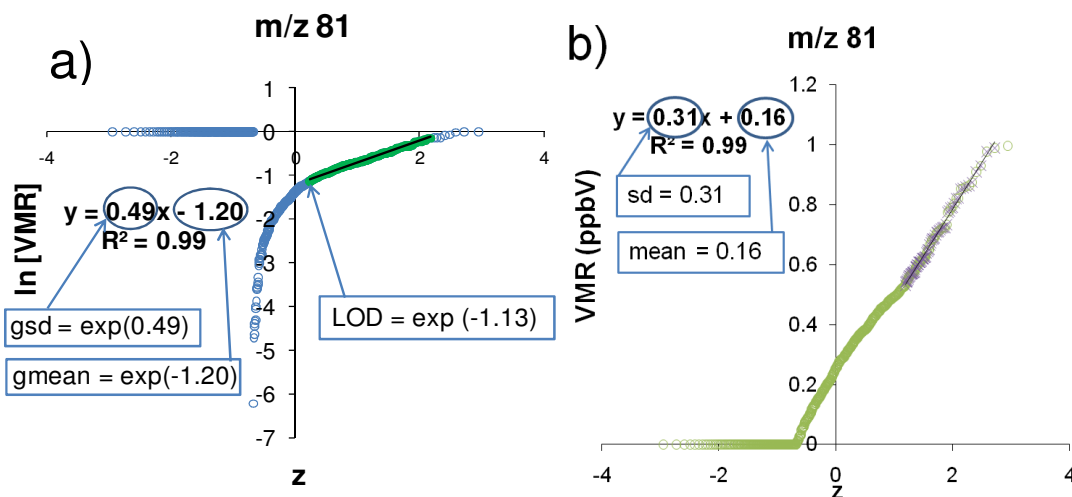
<i>m/z</i>	33	45	59	69	71	75	81	83	93	137	149	205
Compound	Methanol	Acetaldehyde	Acetone	Isoprene	MVK MACR	HA	MT	Hexanals	Toluene	MT	Estragole	SQT
Sensitivity (cps ppbv <sup>-1</sup> )	84.0	72.8	84.8	22.0	38.7*	98.3*	14.6	58.5	52.5*	7.2	12.0*	6.8*

4

#### 5 **SI-4 Graphical method for LODs, standard deviations and means**

6 For the data which had lognormal distribution, common for environmental datasets, the  
 7 exponent of the slope of the lognormal line on a log-probability plot corresponds to the  
 8 geometrical standard deviation (and the exponential of the intercept corresponds to the  
 9 geometrical mean). The geometrical LOD can be found from the exponential of the intercept  
 10 (Helsel, 1990). Similarly, for normally-distributed data, the slope of the line of non-  
 11 logarithmic VMR values versus normal cumulative distributions (*z*) corresponds to the  
 12 arithmetic standard deviation and the intercept to the arithmetic mean. For compounds whose  
 13 distributions turned out to be multimodal (e.g. isoprene, MVK) the graphical methods were  
 14 not applicable. The LODs, standard deviations and means derived by these methods were  
 15 presented in Table 1 of the main text.

16



1

2 Figure S2. An example of the graphical estimation of the limit of detection and other statistical  
 3 parameters from lognormal data values (a) and normal data values (b) plotted against normal  
 4 cumulative distributions. Blue arrows indicate the way to derive geometrical standard deviation (gsd),  
 5 geometrical mean (gmean), limit of detection (LOD), and in case of normal distribution arithmetical  
 6 standard deviation (sd) and arithmetical mean (mean). Graphically derived values are compared with  
 7 calculated values in Table 1 of the main text.

8

### 9 SI-5 Flux derivation and validation

10 PTR-MS, with its relatively high sampling rate, is a perfect tool for application in direct, eddy  
 11 covariance, but when more than one  $m/z$  are monitored sequentially the timeseries are not  
 12 continuous any more, but disjunct. As typically several compounds are selected, the  
 13 instrument can serve as a disjunct sampler, such that the quadrupole analyses one  $m/z$  after  
 14 another during continuous flow. Its use in this manner has been termed ‘virtual disjunct eddy  
 15 covariance’ (vDEC) (Karl, 2002) or ‘continuous flow disjunct eddy covariance’ (cfDEC)  
 16 (Rinne et al., 2008; Rinne et al., 2002); both names denote the same approach. Files  
 17 containing 25-min arrays of wind and PTR-MS data were validated for periods of breakdown  
 18 or other disturbances according to the log file. After a careful examination, no raw data files  
 19 have been marked for despiking or detrending. Double coordinate rotation has been applied to  
 20 the wind speed vectors in order to account for tilts of the anemometer. Each data row  
 21 corresponding to a given VOC was converted to ppbv (as described in Sect. SI-3) and  
 22 subsequently to  $\mu\text{g m}^{-3}$  using instantaneous pressure values from the Vaisala sensor attached  
 23 close to the sonic anemometer. For PTR-MS and wind data, the gaps between PTR-MS rows

1 were filled with “NaN”s in order to align the frequency of the two time series, and the  
 2 covariance function was then obtained by computing separately for each VOC the covariance  
 3 between the instantaneous deviation in mixing ratio ( $\chi'$ ) and the instantaneous deviation in  
 4 vertical wind velocity ( $w'$ ) (i.e.,  $\text{cov}\langle w'\chi'\rangle$ ) for each time lag step (0.05 s) expressed as a  
 5 shift in the wind row versus concentration row. If a clear maximum in the covariance was  
 6 found within the time lag window, which was defined as at least twice the theoretical lag time  
 7 and not less than twice the cycle length, then the time lag was recorded for this 25 min period  
 8 and applied in the final computation of the flux as below:

$$9 \quad F_{VOC} = \sum (w_i - \bar{w}) \times (\chi_{i+\tau} - \bar{\chi})$$

10 (S3)

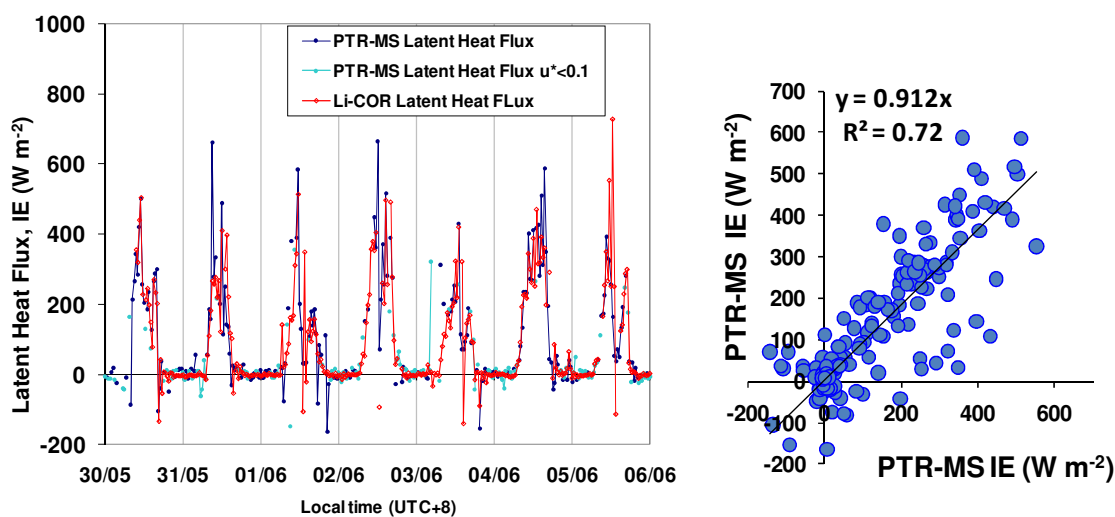
11 where  $w_i$  and  $\bar{w}$  are the instantaneous value and mean over an integration period, respectively,  
 12 for vertical wind velocity,  $\chi_{i+\tau}$  is the lag-time adjusted instantaneous value for the mixing  
 13 ratio and  $\bar{\chi}$  is the mean mixing ratio over the same integration period.

14 The optimum time lag was found automatically from the maximum covariance using a  
 15 LabVIEW program. If no acceptable maximum was found, or if the flux value was below the  
 16 detection limit (defined as 3 times the standard deviation of the covariance for lag times well  
 17 outside the possible window (Spirig et al., 2005), then the data point was marked as invalid  
 18 and was not included in further analysis. Finally, the accepted lag times were manually  
 19 examined in terms of their variability. If the lag time exceeded the theoretical lag time (based  
 20 on sample flow rates) by more than the length of a measurement cycle, or if the lag time  
 21 found from the covariance functions of shorter integration time sub-periods (e.g. 5 min) was  
 22 found variable within the 25 min period, then any peak in the covariance found by the  
 23 program was marked unreal (pseudopeak). However, the lag time value was allowed to be  
 24 variable by not more than 30% within a 25-min period (as found on 5-min integration times).

25 In addition, the data were labelled according to routine tests commonly used in eddy  
 26 covariance for filtering purposes (Clement et al., 2009; Foken and Wichura, 1996; Langford  
 27 et al., 2009a; Moncrieff et al., 1997): the lower limit for the friction velocity was normally set  
 28 to  $0.15 \text{ m s}^{-1}$  and points below this threshold were not included in analyses unless for specific  
 29 tests. According to the FLUXNET criteria for ideal conditions described by Foken et al.  
 30 (2004) the turbulence was quite well developed at the site, with 90 % of data in the first 3

1 classes and no data ranked in 8<sup>th</sup> or 9<sup>th</sup> category. However, at night, friction velocities were  
2 typically below the threshold of  $0.15 \text{ m s}^{-1}$ . According to the recommendations of Foken and  
3 Wichura (1996), data were not included in further analysis if the deviation from the ideal  
4 integral similarity characteristics was higher than 60%, and were labelled lower quality if they  
5 were within 30-60% of the ideal. A stationarity test (the value for the flux integrated over 25  
6 min compared with the average of 5 values of fluxes integrated over 5 min segments of the  
7 same averaging period) was used to exclude non-stationary data when the difference was  
8 above 60% and to label as low quality periods with differences between 30 and 60%. These  
9 tests were done on the sensible heat data and the affected periods were also removed from the  
10 VOC flux datasets.

11 Flux losses associated with signal damping due to residence time in the tubing were assessed  
12 by comparing latent heat fluxes derived from  $m/z$  37, calibrated using specific humidity  
13 converted from relative humidity (Vaisala WXT Weather Transmitter), with latent heat fluxes  
14 from the an open path gas analyser (LI-COR 7500 Infrared Gas Analyser; (Skiba et al.,  
15 2011)). The close agreement (Figure S3) suggested that flux losses due to damping in the  
16 PTR-MS inlet line and due to the internal 1 Hz response time of the PTR-MS were negligible.



17

18 Figure S3. Comparison of latent heat fluxes (IE) derived by PTR-MS and open-path infrared gas  
19 analyser: a) time series b) linear regression.

20

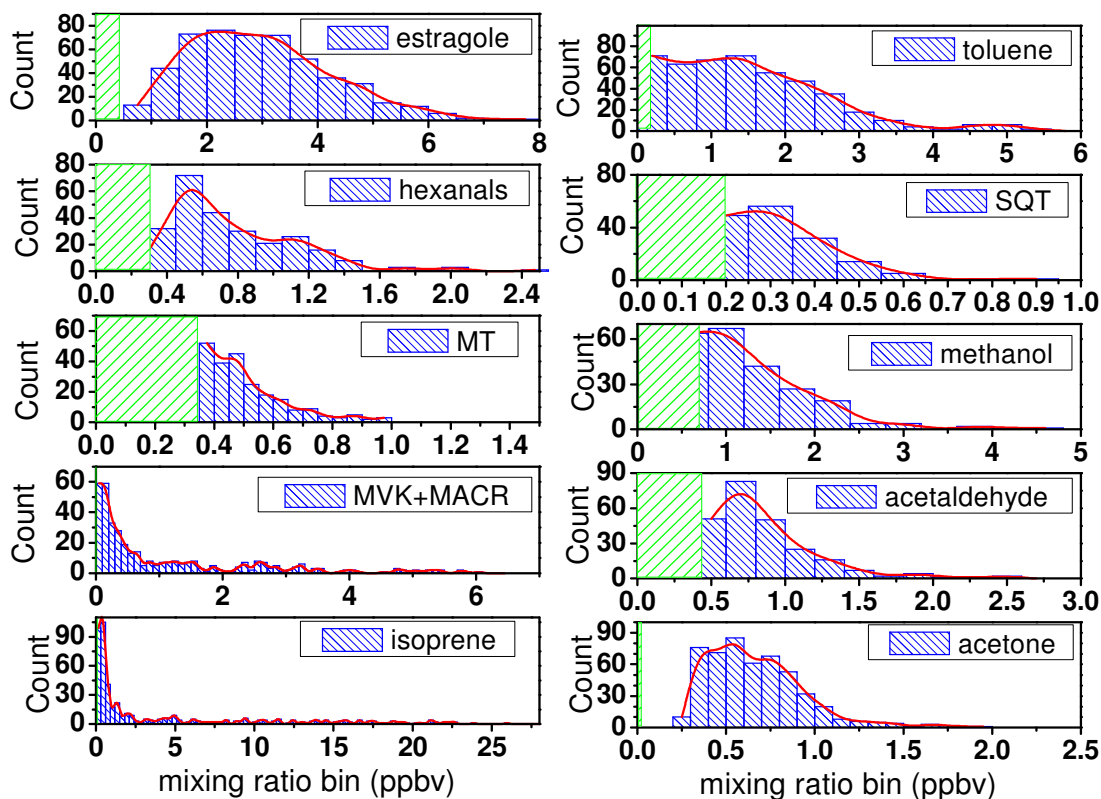
21 Finally, low frequency losses were examined by comparison with fluxes with longer  
22 averaging periods (Langford et al., 2009a) and the error introduced by disjunct sampling was

1 estimated by comparing disjunct series for sensible heat flux (corresponding to times when  
2 PTR-MS data were available) with continuous data for sensible heat flux (Langford et al.,  
3 2009b). The overall flux losses were found to be below 10% and no corrections have been  
4 made. Taking all above into account an average 35 % precision for the flux was estimated.

5

## 6 SI-6 Distributions of mixing ratios

7 Figure S4 shows the frequency distributions of the mixing ratios for the individual VOCs  
8 observed over the oil palm plantation.



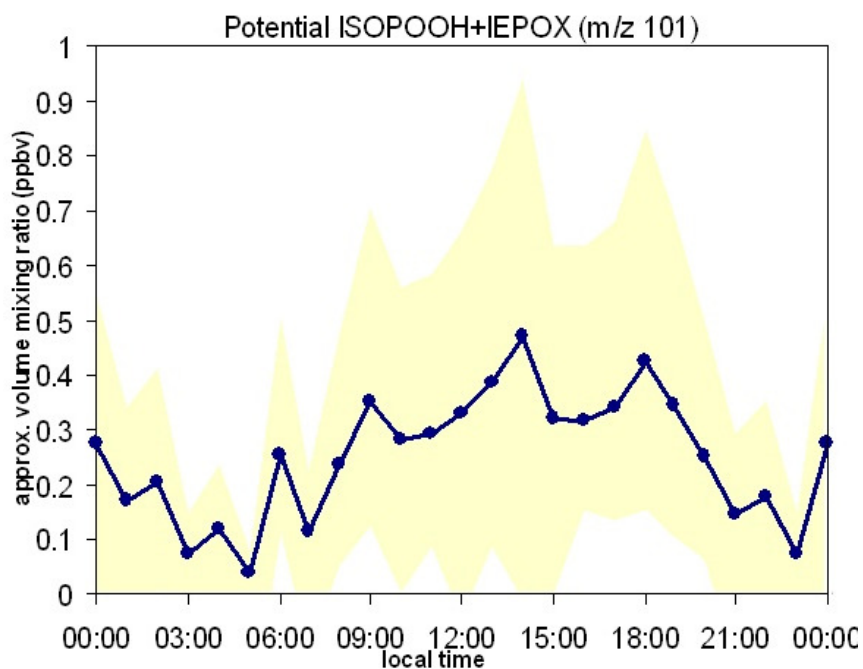
9

10 Figure S4. Distributions of the volume mixing ratio values of the compounds measured in the flux  
11 mode. Green areas correspond to detection limits.

12

## 13 SI-7 Possible isoprene hydroxyhydroperoxides and epoxides

14 Figure S5 shows the approximate mixing ratio of the sum of isoprene peroxides and epoxides  
15 as derived from  $m/z$  101.



1

2 Figure S5. Possible isoprene peroxides and epoxides coinciding at 101 m/z ion channel.

3

#### 4 **SI-8 Comparisons between parameterised and original G06 model**

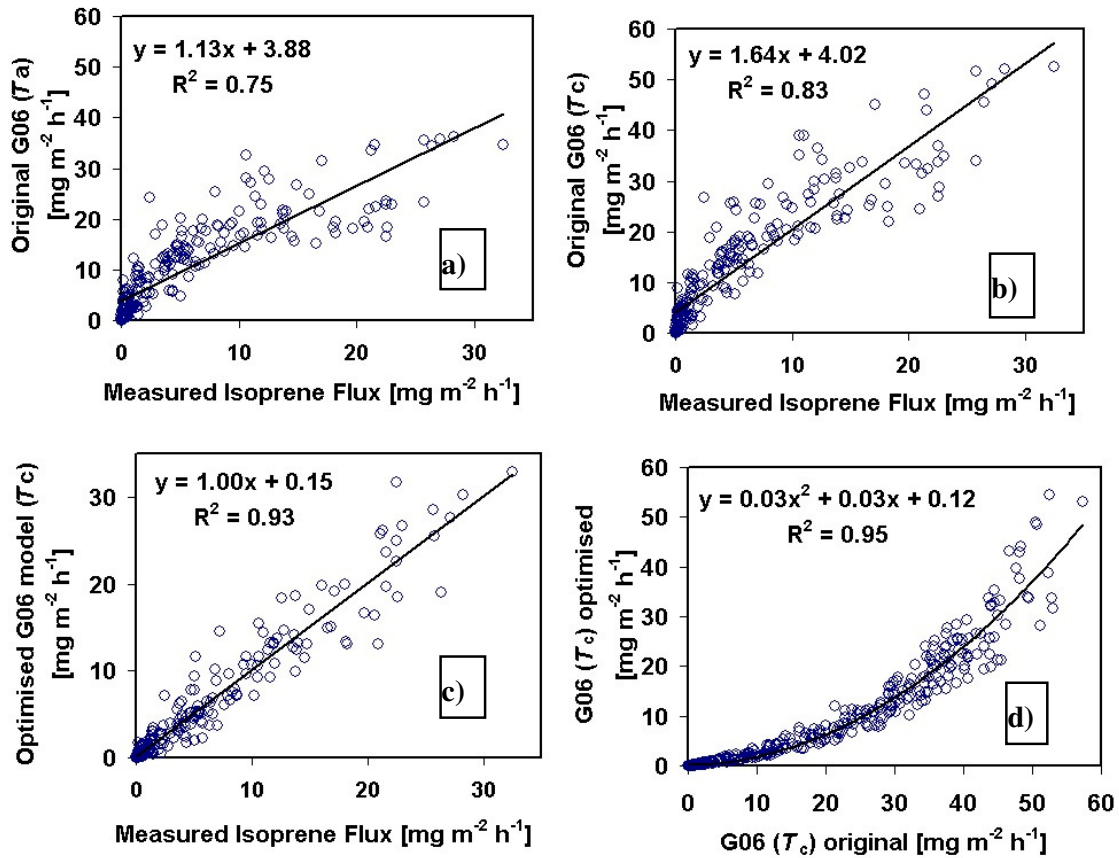
5 The Guenther et al. (2006) model (G06) is the most advanced empirical model for terpene  
6 emission, which is a significant advancement from previous Guenther et al. models (e.g.  
7 Guenther et al., 1995) in that the parameters which used to assume constant values (i.e.,  $\alpha$ ,  $C_p$ ,  
8  $T_{opt}$  and  $E_{opt}$ ) were extended to simulate variations in enzymatic kinetics and isoprene  
9 substrate availability, caused by previous history of temperature and PAR, as tested in a range  
10 of field studies (Geron et al., 2000; Hanson and Sharkey, 2001; Monson et al., 1994; Petron et  
11 al., 2001; Sharkey et al., 1999). Ten empirical parameters have been chosen and labelled  
12 analogously to those in equations presented for estragole emission parameterisation by  
13 Misztal et al. (2010). These equations for the temperature and PAR dependent activity factors  
14 ( $\gamma_T$  and  $\gamma_P$ ) were merged together into one equation so the parameterised flux is represented as  
15 below Eq. (S4) with the 10 parameters marked as b1-b6,  $T_b$ ,  $P_0$ ,  $CT_1$  and  $CT_2$  to be  
16 optimised to fit the experimental data from oil palms. The dependent variables were the  
17 photosynthetically active radiation (PAR) and the canopy temperature (T) estimated from an  
18 ambient temperature using the resistance approach. The P24 and T24 are the 24 h averages of  
19 previous PAR and T, respectively; and P240 and T240 are the previous 10-day averages.

$$F_{G06} = \underbrace{\text{BER} \cdot b_3 \cdot \exp[b_2 \cdot (P_{24} - P_0)] \cdot (P_{240})^{0.6} \cdot \frac{[b_1 - b_2 \ln(P_{240})] \cdot \text{PAR}}{\sqrt{1 + [b_1 - b_2 \ln(P_{240})]^2 \cdot \text{PAR}^2}}}_{\gamma_P} \cdot \underbrace{b_5 \cdot \exp[b_6 \cdot (T_{24} - 297)] \cdot \exp[b_6 \cdot (T_{240} - 297)]}_{\gamma_T} \cdot \frac{C_{T2} \cdot \exp\left[C_{T1} \cdot \left(\frac{1}{T_{\text{opt}}} - \frac{1}{T}\right) \cdot \frac{1}{0.00831}\right]}{C_{T2} - C_{T1} \cdot \left[1 - \exp\left(C_{T2} \cdot \left(\frac{1}{T_{\text{opt}}} - \frac{1}{T}\right) \cdot \frac{1}{0.00831}\right)\right]}$$

(S4)

2 Comparison between the original G06 model using  $T_a(15 \text{ m})$ , measured 3 m above the  
3 canopy, and the measurement is presented in Figure S6a, and the analogous comparison using  
4 the canopy temperature ( $T_c$ ) in the G06 model in Figure S6b. By optimising the G06  
5 parameters based on the measured canopy flux, the model fit improves significantly from  
6 originally  $r^2 = 0.75$  to 0.91, if a constant basal emission rate (BER) and  $T_a(15 \text{ m})$  are used (not  
7 shown). Replacing  $T_a(15 \text{ m})$  for  $T_c$  in the original model increases the coefficient of  
8 determination to 0.83 (Figure S6b) which after parameter adjustment improves further to 0.93  
9 (Figure S6c). The corresponding time series are almost identical. The comparison of the  
10 original and the parameterised G06 model outputs for oil palms has a quadratic relationship  
11 (Figure S6d), which suggests that the original model underestimates the emission at moderate  
12 temperatures and light levels. For the adjusted BER, the original G06 has a tendency to  
13 overestimate the small flux region (morning, afternoon) while underestimating the high fluxes  
14 (noon) in comparison with the 1:1 slope with measurement.

15

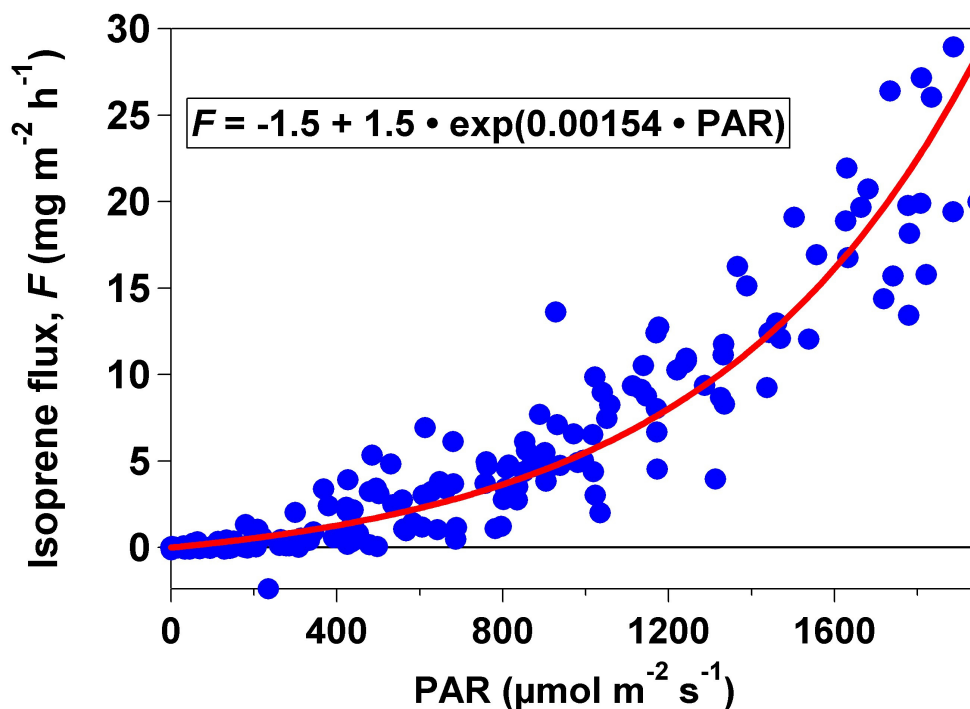


1

2 Figure S6 Comparison of measured fluxes with the original G06 using ambient temperature at a  
 3 constant BER of  $12.8 \text{ mg m}^{-2} \text{ h}^{-1}$  (a), with the original G06 using canopy temperature at a constant  
 4 BER of  $12.8 \text{ mg m}^{-2} \text{ h}^{-1}$  (b), and the parameterised G06 optimised for oil palm plantation using canopy  
 5 temperature at a constant BER of  $22.8 \text{ mg m}^{-2} \text{ h}^{-1}$  (c). The relationship between original and optimised  
 6 G06 model is shown in (d).

### 7 SI-9 Isoprene response to PAR

8 Figure S7 shows isoprene emission in response to PAR derived from PTR-MS canopy  
 9 measurements. The curve is getting much steeper after  $1000 \mu\text{mol m}^{-2} \text{ s}^{-1}$ . The relationship  
 10 with temperature was presented in the main text.(Figure 7)



1

2 Figure S7. Relationship between isoprene flux measured above oil palm canopy and PAR.

3

#### 4 References

- 5 Clement, R. J., Burba, G. G., Grelle, A., Anderson, D. J., and Moncrieff, J. B.: Improved trace  
 6 gas flux estimation through IRGA sampling optimization, *Agricultural and Forest*  
 7 *Meteorology*, 149, 623-638, 10.1016/j.agrformet.2008.10.008, 2009.
- 8 Davison, B., Taipale, R., Langford, B., Misztal, P., Fares, S., Matteucci, G., Loreto, F., Cape,  
 9 J. N., Rinne, J., and Hewitt, C. N.: Concentrations and fluxes of biogenic volatile organic  
 10 compounds above a Mediterranean macchia ecosystem in western Italy, *Biogeosciences*, 6,  
 11 1655-1670, 2009.
- 12 Foken, T., and Wichura, B.: Tools for quality assessment of surface-based flux measurements,  
 13 *Agricultural and Forest Meteorology*, 78, 83-105, 1996.
- 14 Foken, T., Göckede, M., Mauder, M., Mahrt, L., Amiro, B., and Munger, W.: Post-field data  
 15 quality control, in: *Handbook of Micrometeorology: A guide for surface flux measurement*  
 16 *and analysis.*, edited by: Lee, W. M. X., and Law, B., Kluwer Academic Publishers,  
 17 Dordrecht, 181-203, 2004.
- 18 Geron, C., Guenther, A., Sharkey, T., and Arnts, R. R.: Temporal variability in basal isoprene  
 19 emission factor, *Tree Physiology*, 20, 799-805, 2000.
- 20 Guenther, A., Hewitt, C. N., Erickson, D., Fall, R., Geron, C., Graedel, T., Harley, P.,  
 21 Klinger, L., Lerdau, M., McKay, W. A., Pierce, T., Scholes, B., Steinbrecher, R., Tallamraju,  
 22 R., Taylor, J., and Zimmerman, P.: A global-model of natural volatile organic-compound  
 23 emissions, *Journal of Geophysical Research-Atmospheres*, 100, 8873-8892, 1995.

- 1 Guenther, A., Karl, T., Harley, P., Wiedinmyer, C., Palmer, P. I., and Geron, C.: Estimates of  
2 global terrestrial isoprene emissions using MEGAN (Model of Emissions of Gases and  
3 Aerosols from Nature), *Atmos. Chem. Phys. Discuss.*, 6, 107-173, 2006.
- 4 Hanson, D. T., and Sharkey, T. D.: Rate of acclimation of the capacity for isoprene emission  
5 in response to light and temperature, *Plant Cell and Environment*, 24, 937-946, 2001.
- 6 Helsel, D. R.: Less than obvious - statistical treatment of data below the detection limit,  
7 *Environmental Science & Technology*, 24, 1766-1774, 1990.
- 8 Karl, T. G., C. Spirig, et al.: Virtual disjunct eddy covariance measurements of organic  
9 compound fluxes from a subalpine forest using proton transfer reaction mass spectrometry,  
10 *Atmospheric Chemistry and Physics*, 2, 279-291, 2002.
- 11 Kim, S., Karl, T., Helmig, D., Daly, R., Rasmussen, R., and Guenther, A.: Measurement of  
12 atmospheric sesquiterpenes by proton transfer reaction-mass spectrometry (PTR-MS), *Atmos.*  
13 *Meas. Tech.*, 2, 99-112, 2009.
- 14 Kuhn, U., Andreae, M. O., Ammann, C., Araujo, A. C., Brancaleoni, E., Ciccioli, P., Dindorf,  
15 T., Frattoni, M., Gatti, L. V., Ganzeveld, L., Kruijt, B., Lelieveld, J., Lloyd, J., Meixner, F.  
16 X., Nobre, A. D., Poschl, U., Spirig, C., Stefani, P., Thielmann, A., Valentini, R., and  
17 Kesselmeier, J.: Isoprene and monoterpene fluxes from Central Amazonian rainforest inferred  
18 from tower-based and airborne measurements, and implications on the atmospheric chemistry  
19 and the local carbon budget, *Atmospheric Chemistry and Physics*, 7, 2855-2879, 2007.
- 20 Langford, B., Davison, B., Nemitz, E., and Hewitt, C. N.: Mixing ratios and eddy covariance  
21 flux measurements of volatile organic compounds from an urban canopy (Manchester, UK),  
22 *Atmos. Chem. Phys.*, 9, 1971-1987, 2009a.
- 23 Langford, B., Nemitz, E., House, E., Phillips, G. J., Famulari, D., Davison, B., Hopkins, J. R.,  
24 Lewis, A. C., and Hewitt, C. N.: Fluxes and concentrations of volatile organic compounds  
25 above central London, UK, *Atmos. Chem. Phys. Discuss.*, 9, 17297-17333, 2009b.
- 26 Misztal, P. K., Owen, S. M., Guenther, A. B., Rasmussen, R., Geron, C., Harley, P., Phillips,  
27 G. J., Ryan, A., Edwards, D. P., Hewitt, C. N., Nemitz, E., Siong, J., Heal, M. R., and Cape, J.  
28 N.: Large estragole fluxes from oil palms in Borneo, *Atmos. Chem. Phys.*, 10, 4343-4358,  
29 10.5194/acp-10-4343-2010, 2010.
- 30 Moncrieff, J., Valentini, R., Greco, S., Guenther, S., and Ciccioli, P.: Trace gas exchange over  
31 terrestrial ecosystems: methods and perspectives in micrometeorology, *J. Exp. Bot.*, 48, 1133-  
32 1142, 10.1093/jxb/48.5.1133, 1997.
- 33 Monson, R. K., Harley, P. C., Litvak, M. E., Wildermuth, M., Guenther, A. B., Zimmerman,  
34 P. R., and Fall, R.: Environmental and developmental controls over the seasonal pattern of  
35 isoprene emission from aspen leaves, *Oecologia*, 99, 260-270, 1994.
- 36 Nemitz, E., Loubet, B., Lehmann, B. E., Cellier, P., Neftel, A., Jones, S. K., Hensen, A., Ihly,  
37 B., Tarakanov, S. V., and Sutton, M. A.: Turbulence characteristics in grassland canopies and  
38 implications for tracer transport, *Biogeosciences*, 6, 1519-1537, 2009.
- 39 Petron, G., Harley, P., Greenberg, J., and Guenther, A.: Seasonal temperature variations  
40 influence isoprene emission, *Geophysical Research Letters*, 28, 1707-1710, 2001.
- 41 Rinne, J., Durand, P., and Guenther, A.: An airborne disjunct eddy covariance system:  
42 Sampling strategy and instrument design, 15th Symposium on Boundary Layers and  
43 Turbulence, 151-154, 2002.

- 1 Rinne, J., Douffet, T., Prigent, Y., and Durand, P.: Field comparison of disjunct and  
2 conventional eddy covariance techniques for trace gas flux measurements, *Environmental*  
3 *Pollution*, 152, 630-635, 2008.
- 4 Sharkey, T. D., Singsaas, E. L., Lerdau, M. T., and Geron, C. D.: Weather effects on isoprene  
5 emission capacity and applications in emissions algorithms, *Ecological Applications*, 9, 1132-  
6 1137, 1999.
- 7 Skiba, U. M., Siong, J., Helfter, C., Di Marco, C., Linatoc, A., Fowler, D., and Nemitz, E.:  
8 Greenhouse gas (N<sub>2</sub>O, CH<sub>4</sub> and CO<sub>2</sub>) exchange with contrasting land uses in SE Asia,  
9 *Atmos. Chem. Phys. Discuss.*, in preparation for submission, 2011.
- 10 Spirig, C., Neftel, A., Ammann, C., Dommen, J., Grabmer, W., Thielmann, A., Schaub, A.,  
11 Beauchamp, J., Wisthaler, A., and Hansel, A.: Eddy covariance flux measurements of  
12 biogenic VOCs during ECHO 2003 using proton transfer reaction mass spectrometry,  
13 *Atmospheric Chemistry and Physics*, 5, 465-481, 2005.
- 14 Steinbacher, M., Dommen, J., Ammann, C., Spirig, C., Neftel, A., and Prevot, A. S. H.:  
15 Performance characteristics of a proton-transfer-reaction mass spectrometer (PTR-MS)  
16 derived from laboratory and field measurements, *International Journal of Mass Spectrometry*,  
17 239, 117-128, 2004.
- 18 Taipale, R., Ruuskanen, T. M., Rinne, J., Kajos, M. K., Hakola, H., Pohja, T., and Kulmala,  
19 M.: Technical Note: Quantitative long-term measurements of VOC concentrations by PTR-  
20 MS - measurement, calibration, and volume mixing ratio calculation methods, *Atmospheric*  
21 *Chemistry and Physics*, 8, 6681-6698, 2008.
- 22 Tani, A., Hayward, S., and Hewitt, C. N.: Measurement of monoterpenes and related  
23 compounds by proton transfer reaction-mass spectrometry (PTR-MS), *International Journal of*  
24 *Mass Spectrometry*, 223, 561-578, 2003.
- 25 Tani, A., Hayward, S., Hansel, A., and Hewitt, C. N.: Effect of water vapour pressure on  
26 monoterpene measurements using proton transfer reaction-mass spectrometry (PTR-MS),  
27 *International Journal of Mass Spectrometry*, 239, 161-169, 2004.
- 28 Warneke, C., van der Veen, C., Luxembourg, S., de Gouw, J. A., and Kok, A.: Measurements  
29 of benzene and toluene in ambient air using proton-transfer-reaction mass spectrometry:  
30 calibration, humidity dependence, and field intercomparison, *International Journal of Mass*  
31 *Spectrometry*, 207, 167-182, 2001.
- 32 Zhao, J., and Zhang, R.: Proton transfer reaction rate constants between hydronium ion  
33 (H<sub>3</sub>O<sup>+</sup>) and volatile organic compounds, *Atmospheric Environment*, 38, 2177-2185, 2004.
- 34
- 35